Metabolic control analysis of hepatic glycogen synthesis in vivo

Yuichi Nozaki[a,b], Max C. Petersen[a,c], Dongyan Zhang[a], Daniel F. Vatner[a], Rachel J. Perry[a,c], Abudukadier Abulizi[a], Sofie Haedersdal[a,d,e], Xian-Man Zhang[a], Gina M. Butrico[a], Varman T. Samuel[a,f], Graeme F. Mason[g,h], Gary W. Cline[a], Kitt F. Petersen[a], Douglas L. Rothman[d,i], and Gerald I. Shulman[a,c,1]

[a]Department of Internal Medicine, Yale School of Medicine, New Haven, CT 06520; [b]Department of Gastroenterology and Hepatology, National Center for Global Health and Medicine, 1628655 Tokyo, Japan; [c]Department of Cellular & Molecular Physiology, Yale School of Medicine, New Haven, CT 06520; [d]Center for Clinical Metabolic Research, Gentofte and Herlev Hospital, 2900 Hellerup, Denmark; [e]Type 2 Biology, Steno Diabetes Center Copenhagen, 2820 Gentofte, Denmark; [f]Department of Medicine, Veterans Affairs Medical Center, West Haven, CT 06516; [g]Department of Radiology and Biomedical Imaging, Yale School of Medicine, New Haven, CT 06520; [h]Department of Psychiatry, Yale School of Medicine, New Haven, CT 06520; and [i]Department of Biomedical Engineering, Yale School of Medicine, New Haven, CT 06520

Multiple insulin-regulated enzymes participate in hepatic glycogen synthesis, and the rate-controlling step responsible for insulin stimulation of glycogen synthesis is unknown. We demonstrate that glucokinase (GCK)-mediated glucose phosphorylation is the rate-controlling step in insulin-stimulated hepatic glycogen synthesis in vivo, by use of the somatostatin pancreatic clamp technique using [$^{13}C_6$]glucose with metabolic control analysis (MCA) in three rat models: 1) regular chow (RC)-fed male rats (control), 2) high fat diet (HFD)-fed rats, and 3) RC-fed rats with portal vein glucose delivery at a glucose infusion rate matched to the control. During hyperinsulinemia, hyperglycemia dose-dependently increased hepatic glycogen synthesis. At similar levels of hyperinsulinemia and hyperglycemia, HFD-fed rats exhibited a decrease and portal delivery rats exhibited an increase in hepatic glycogen synthesis via the direct pathway compared with controls. However, the strong correlation between liver glucose-6-phosphate concentration and net hepatic glycogen synthetic rate was nearly identical in these three groups, suggesting that the main difference between models is the activation of GCK. MCA yielded a high control coefficient for GCK in all three groups. We confirmed these findings in studies of hepatic GCK knockdown using an antisense oligonucleotide. Reduced liver glycogen synthesis in lipid-induced hepatic insulin resistance and increased glycogen synthesis during portal glucose infusion were explained by concordant changes in translocation of GCK. Taken together, these data indicate that the rate of insulin-stimulated hepatic glycogen synthesis is controlled chiefly through GCK translocation.

metabolic control analysis | hepatic glycogen synthesis | in vivo | glucokinase | hepatic insulin resistance

Stimulation of net hepatic glycogen synthesis is one of the major direct effects of insulin on the hepatocyte and an important mechanism for insulin suppression of hepatic glucose production (1). Hepatic glycogen can be synthesized from glucose directly (glucose to glucose-6-phosphate [G6P] to uridine diphosphate [UDP]-glucose to glycogen) or indirectly (glucose to G6P to pyruvate to G6P to UDP-glucose to glycogen) (2). Multiple insulin-regulated enzymes participate in hepatic glycogen synthesis; these include glucokinase (GCK), which controls the initial step of glucose phosphorylation, and glycogen synthase (GSase), which catalyzes the final step of incorporation into glycogen. The activities of these enzymes are coordinately increased by insulin but are also subject to multimodal control—transcriptional, allosteric, phosphorylation, and protein–protein interactions—by glucose, insulin, glucagon, and other inputs. In the setting of this complexity, the rate-controlling step responsible for insulin stimulation of hepatic glycogen synthetic flux in vivo is not well established.

GCK is essential for whole-body glucose homeostasis (3); however, its relative contribution to control of insulin-stimulated hepatic glycogen synthesis is uncertain. GCK is transcriptionally up-regulated by insulin through an incompletely described AKT- and SREBP1-dependent mechanism, but GCK activity is thought to be primarily regulated by posttranslational control of its subcellular localization. Hepatic GCK activity is regulated by GCK regulatory protein (GKRP), which competes with glucose to bind and inactivate GCK in the nucleus. In the postprandial, high-glucose state, GKRP releases GCK to the cytoplasm, where it is active (4, 5).

Metabolic control analysis (MCA) has been developed to quantitatively describe the sharing of flux control through a metabolic pathway by the enzymes in the pathway (6, 7). As described in *Methods*, the flux control coefficient of an enzyme can be measured by selectively altering the activity of the enzyme while maintaining constant activities of other enzymes in the pathway (8). MCA has been used for diverse applications. For example, MCA revealed that control of insulin-stimulated muscle glycogen synthesis occurs at the level of glucose transport (GT)/phosphorylation (8), presaging detailed elucidation of the molecular mechanisms for insulin-stimulated myocellular GLUT4 translocation. Agius and coworkers (9) employed MCA in combination with a specific phosphorylase inhibitor in isolated hepatocytes and concluded that phosphorylase is a strong candidate target for controlling hyperglycemia in type 2 diabetes (T2D) in both absorptive and postabsorptive states.

Significance

Hepatic glycogen synthesis plays a critical role in maintaining normal glucose homeostasis; however, the rate-controlling step regulating this process is unknown. Applying metabolic control analysis in vivo, we show that the regulation of insulin-stimulated hepatic glycogen synthesis under both normal and pathophysiological conditions of fatty liver-associated hepatic insulin resistance is controlled at the glucokinase (GCK) step through GCK translocation.

Insulin-stimulated hepatic glycogen synthesis has been reported to be impaired in lipid-induced hepatic insulin resistance during hyperinsulinemic–hyperglycemic clamp studies (1, 10) and to be augmented by portal glucose infusion (11). However, the mechanisms by which this occurs in vivo have not been fully elucidated.

In this study, we investigated the nature of rate control for insulin-stimulated hepatic glycogen synthesis in vivo, employing MCA in rats subjected to somatostatin pancreatic clamps at various plasma insulin and glucose concentrations. To examine the mechanisms of lipid-induced hepatic insulin resistance to glycogen synthesis, we also studied rats fed a high-fat diet (HFD). Finally, to investigate the nature of the "portal factor," the preferential activation of glycogen synthesis in response to portal vein glucose, we studied regular chow (RC)-fed rats with portal vein glucose delivery at glucose infusion rates matched to rats with similar peripheral glucose infusion rates.

Results

Somatostatin Pancreatic Clamps. To examine hepatic glycogen synthesis under physiological conditions of varying plasma insulin and glucose concentrations, we employed somatostatin pancreatic clamps in rats (not just RC; see the groups listed below) in which somatostatin was infused to suppress endogenous insulin and glucagon. Insulin was infused at rates of 0.5 (basal replacement) or 4.0 (hyperinsulinemia) mU/(kg·min). Glucose, including uniformly labeled $^{13}C_6$ glucose ($[^{13}C_6]$ glucose) as a tracer, was infused to maintain one of three target plasma glucose concentrations: euglycemia (100 mg/dL), hyperglycemia (180 mg/dL), or marked hyperglycemia (300 mg/dL). We studied five permutations of plasma insulin and glucose target levels: group 1, low insulin/euglycemia; group 2, low insulin/hyperglycemia; group 3, high insulin/euglycemia; group 4, high insulin/hyperglycemia; and group 5, high insulin/marked hyperglycemia. These five groups were studied in each of in three models: RC-fed rats (control), insulin-resistant rats fed an HFD for 3 d, and RC-fed rats in which glucose was infused through the portal vein at rates matched to those used in the control cohort (portal delivery). In the HFD groups, we studied another permutation of high insulin and marked hyperglycemia (400 mg/dL). Clamp studies were limited to 90 min, ending prior to somatostatin tachyphylaxis.

Control RC-fed model vs. HFD-fed model. There was no significant difference in rat body weight between groups (Table 1). Plasma glucose concentrations and glucose infusion rates were similar between control and HFD groups (*SI Appendix*, Fig. S1 *A* and *B*) during the clamp experiments. Somatostatin effectively suppressed endogenous rat insulin secretion as reflected by undetectable plasma C-peptide concentrations; plasma human insulin concentrations were ~8 μU/mL with the 0.5 mU/(kg·min) insulin infusion and ~80 μU/mL with the 4.0 mU/(kg·min) insulin infusion (Table 1).

Portal delivery model. Body weight, plasma glucose concentration, glucose infusion rate, plasma human insulin, and rat C-peptide concentrations were similar between portal delivery rats and sham portal vein catheterization control rats (*SI Appendix*, Fig. S1 *C* and *D* and Table 2).

Hepatic Glycogen Concentration and Total Glycogen Synthetic Rate.
Control RC-fed model vs. HFD-fed model. In control rats receiving basal insulin replacement, hyperglycemia did not stimulate net hepatic glycogen synthesis. In contrast, control rats subjected to both hyperinsulinemia and hyperglycemia displayed progressively increased net hepatic glycogen synthetic rate in a glucose dose-dependent manner (Fig. 1). Similarly, under conditions of hyperinsulinemia, hyperglycemia increased hepatic glycogen concentration in a glucose dose-dependent manner (*SI Appendix*, Fig. S2A). Most of the increases in glycogen synthetic rate could be attributed to increases in glycogen synthesis via the direct pathway.

HFD-fed rats exhibited an approximately twofold increase in liver triglyceride (TG) content compared with controls (Table 1). Insulin-stimulated liver AKT2 phosphorylation in postclamp samples was significantly decreased in the HFD group compared to controls in both euglycemic and hyperglycemic groups (*SI Appendix*, Fig. S3), consistent with lipid-induced hepatic insulin resistance as previously described in 3-d HFD-fed male rats (12).

HFD-fed rats subjected to both hyperinsulinemia and hyperglycemia exhibited an increase in both hepatic glycogen concentration and net hepatic glycogen synthetic rate in a glucose dose-dependent manner. At plasma glucose levels of 180 mg/dL or 300 mg/dL and hyperinsulinemia, both total hepatic glycogen concentrations and net hepatic glycogen synthetic rates were significantly decreased in HFD-fed rats compared with controls (Fig. 1 and *SI Appendix*, Fig. S2A).

Portal delivery model. Under conditions of hyperinsulinemia, glucose dose-dependently increased hepatic glycogen synthesis in both portal delivery and control rats (*SI Appendix*, Fig. S4 *A* and *B*). At hyperinsulinemia and glycemia of 100 mg/dL or

Table 1. Characteristics of somatostatin pancreatic clamps in control vs. HFD group cohort (*n* = 3 to 13 per group)

	RC					HFD					High insulin/marked hyperglycemia (400 mg/dL)
	Group 1	Group 2	Group 3	Group 4	Group 5	Group 1	Group 2	Group 3	Group 4	Group 5	
Body weight, g	400 ± 10	421 ± 7	411 ± 14	423 ± 8	417 ± 9	406 ± 7	404 ± 5	409 ± 8	412 ± 6	406 ± 5	401 ± 16
Liver TG concentration, mg/g tissue	7 ± 1	8 ± 1	7 ± 1	7 ± 1	8 ± 1	17 ± 1	19 ± 2	19 ± 3	17 ± 4	17 ± 1	18 ± 2
Plasma insulin, μU/mL											
0 min	0.0 ± 0.0	0.0 ± 0.0	0.0 ± 0.0	0.0 ± 0.0	0.0 ± 0.0	0.0 ± 0.0	0.0 ± 0.0	0.0 ± 0.0	0.0 ± 0.0	0.0 ± 0.0	0.0 ± 0.0
30 min	6.0 ± 0.3	6.0 ± 0.4	72 ± 6	73 ± 3	73 ± 4	6.4 ± 2.2	6.6 ± 0.6	73 ± 2	71 ± 4	74 ± 3	75 ± 12
90 min	8.2 ± 1.0	8.3 ± 0.9	83 ± 8	80 ± 4	86 ± 6	8.3 ± 1.9	8.8 ± 1.4	82 ± 3	79 ± 6	80 ± 4	82 ± 4
Plasma rat C-peptide, pM											
0 min	453 ± 47	431 ± 89	475 ± 19	477 ± 99	490 ± 75	502 ± 81	471 ± 44	538 ± 66	477 ± 54	539 ± 35	494 ± 68
90 min	1 ± 1	3 ± 3	7 ± 7	1 ± 1	5 ± 4	1 ± 1	10 ± 6	2 ± 2	2 ± 1	3 ± 2	1 ± 1

Nozaki et al.

www.manaraa.com

Table 2. Characteristics of somatostatin pancreatic clamps in peripheral and portal glucose infusion model cohort (n = 3 to 18 per group)

	Peripheral glucose infusion					Portal glucose infusion				
	Group 1	Group 2	Group 3	Group 4	Group 5	Group 1	Group 2	Group 3	Group 4	Group 5
Body weight, g	396 ± 9	399 ± 21	380 ± 18	408 ± 6	398 ± 8	399 ± 10	395 ± 15	384 ± 4	408 ± 8	401 ± 5
Plasma insulin, μU/mL										
0 min	0.0 ± 0.0	0.0 ± 0.0	0.0 ± 0.0	0.0 ± 0.0	0.0 ± 0.0	0.0 ± 0.0	0.0 ± 0.0	0.0 ± 0.0	0.0 ± 0.0	0.0 ± 0.0
30 min	6.7 ± 1.2	6.9 ± 1.1	72 ± 6	77 ± 6	75 ± 4	6.8 ± 0.9	7.0 ± 0.5	72 ± 4	76 ± 6	74 ± 9
90 min	8.4 ± 0.4	8.3 ± 0.7	83 ± 6	84 ± 5	81 ± 3	8.2 ± 0.7	7.8 ± 0.6	81 ± 3	84 ± 3	83 ± 5
Plasma rat C-peptide, pM										
0 min	426 ± 5	423 ± 38	435 ± 29	424 ± 22	440 ± 23	435 ± 18	455 ± 36	425 ± 11	416 ± 20	431 ± 24
90 min	5 ± 3	5 ± 5	7 ± 2	8 ± 4	6 ± 3	10 ± 1	8 ± 6	3 ± 2	7 ± 4	5 ± 1

180 mg/dL, both the hepatic glycogen concentration and net liver glycogen synthetic rate were significantly increased in the portal delivery rats compared with the respective controls. However, this was not observed at 300 mg/dL glucose (*SI Appendix*, Fig. S4 *A* and *B*).

Hepatic G6P Concentrations.
Control RC-fed model vs. HFD-fed model. In both control and HFD-fed rats, under conditions of hyperinsulinemia, hyperglycemia increased hepatic G6P concentrations in a glucose-dependent manner. However, under hyperinsulinemic and hyperglycemic conditions (at both 180 and 300 mg/dL glucose), hepatic G6P concentrations were ~25% lower in HFD rats compared with controls (*SI Appendix*, Fig. S2*B*).
Portal delivery model. In parallel with the pattern observed for glycogen synthetic flux, portal delivery of glucose further increased hepatic G6P concentration relative to peripheral IV infusion, and it was significantly higher when plasma glucose concentrations were clamped at 100 and 180 mg/dL (*SI Appendix*, Fig. S4*C*).

Dependence of the Direct Pathway and Total Glycogen Synthesis on Glucose and Insulin Concentration. In order to assess the influence of glucose and insulin concentration on the direct pathway of glycogen synthesis, we used [$^{13}C_6$] glucose in conjunction with gas chromatography–mass spectrometry (MS) analysis to calculate the rate of the direct and indirect pathway of glycogen synthesis for all groups.

In Figs. 2*A* and 3*A* we show the rate of hepatic glycogen synthesis through the direct pathway as a function of glucose and insulin stimulation. For RC rats the relationship is highly sigmoidal with almost no direct pathway synthesis at a glucose concentration of 100 mg/dL. For HFD-fed rats a sigmoidal relationship is also seen but there is a substantial reduction at all glucose levels in the rate of the direct pathway (Fig. 2*A*). This reduction in the direct pathway accounts for almost all of the reduction in total glycogen synthesis rate in the HFD-fed animals. For portal delivery of glucose, a sigmoidal relationship is also seen but there is a substantial increase in the rate of the direct pathway (Fig. 3*A*).

Hepatic G6P Concentration as Predictor of Liver Glycogen Synthesis. We next examined the relationship between liver G6P concentration and the net hepatic glycogen synthetic rate. We calculated the in vivo kinetic parameters using the equation of Palm et al. (13) to determine the best-fit parameter to the curve of total glycogen synthesis vs. G6P concentration. Uncertainties in the fitted parameters were assessed using a Monte Carlo approach (14, 15). As shown in the figures there is an excellent fit of the model to the data from the RC experiments (Figs. 2*B* and 3*B*). Thus, we examined the goodness of fit for the glycogen synthesis vs. G6P curve using the kinetic parameters calculated

from the RC animals. We found an excellent fit to the data in both cases. Finally, as shown in Figs. 2*B* and 3*B*, we combined the data from all studies and determined the best-fit parameters.

The data showed that the kinetic relationship between G6P and glycogen synthetic rate was similar between RC and HFD-fed rats. This relationship was similarly close in rats that underwent both portal and peripheral glucose infusion. Thus, these data suggest that the main differentiating step between these models is the conversion of glucose to G6P via GCK.

MCA of Hepatic Glycogen Synthesis. We employed MCA in our model of insulin-stimulated hepatic glycogen synthesis to determine quantitatively the contributions of the direct pathway, the indirect pathway, and the relative contributions of the individual enzymatic steps to the control of the flux of these pathways. The calculated values of response coefficients (R), flux control coefficients (C), and elasticities (ε) are shown in Table 3. As described in *Methods*, the C value is the relative steady state change
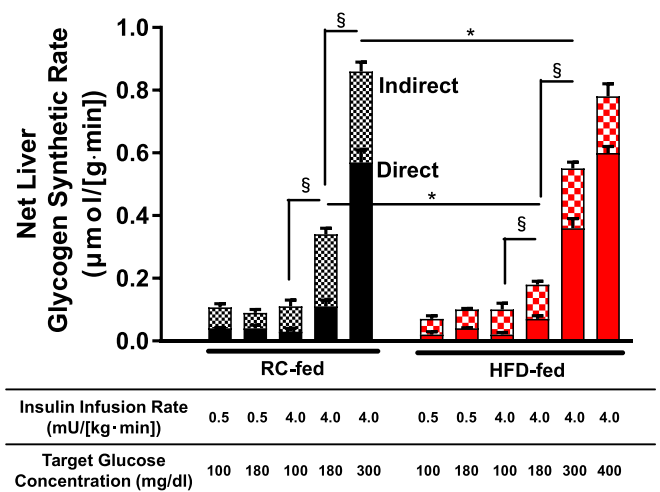

Fig. 1. Net liver glycogen synthetic rate through both direct and indirect pathways in control and HFD rat models. Rats were fed either RC (black bars) or 3-d HFD (red bars) and subjected to somatostatin pancreatic clamps at the insulin infusion rates and target plasma glucose levels listed below the *x* axis. Net hepatic glycogen synthetic rates are represented in the bar graph; the solid part of the bar represents direct pathway synthesis and the checkered part of the bar represents indirect pathway synthesis. Data are the mean ± SEM of n = 3 to 13 per group. Statistical analysis reported for comparisons of net glycogen synthetic rates. Within a diet group (RC- or HFD-fed), all groups were compared with all other groups, with statistics by ANOVA with post hoc testing. Between diet groups, rats subject to identical infusion strategies were compared, with statistics by unpaired Student's *t* test. *P < 0.05 by unpaired Student's *t* test and §P < 0.05 by ANOVA followed by post hoc test.

Nozaki et al.

www.manaraa.com
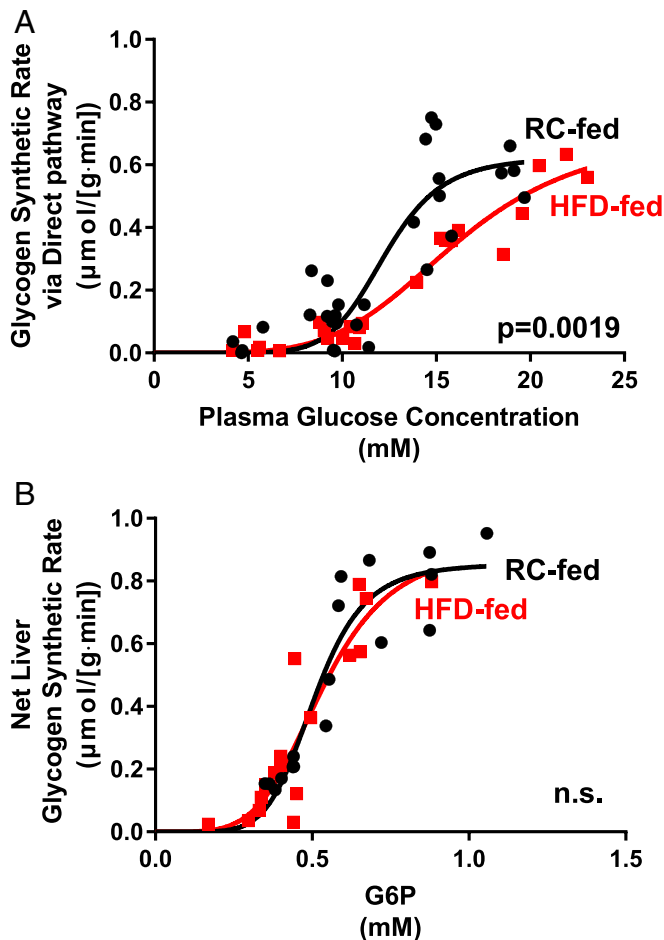
Fig. 2. The relationship between plasma glucose and direct pathway synthesis is altered while net glycogen synthesis vs. hepatic G6P content is unchanged in hepatic insulin resistance. (*A*) Under hyperinsulinemic conditions (4 mU/kg·min), direct pathway glycogen synthetic rate plotted against plasma glucose concentration. Black circles: RC-fed control rats; red squares: HFD-fed rats. (*B*) Under hyperinsulinemic conditions (4 mU/kg·min), net hepatic glycogen synthesis plotted against hepatic G6P content. Black circles: RC-fed control rats; red squares: HFD-fed rats. Data fit to a sigmoidal model. n.s., not significant.

in the flux of the pathway in response to a relative change in an enzyme activity. The ε value is the local response of an enzyme to changes in substrate, product, and allosteric effector concentration. The R value is the effect of an external constant metabolite, in this case glucose, on the pathway flux. We calculated the flux control coefficients for the system by experimentally measuring the value of R and ε from the flux and G6P measurements made at different glucose concentrations. Here, the direct pathway is largely controlled by GCK. The R value for GCK via the direct pathway during hyperinsulinemia was 2.52 ± 2.27 at the glycemic range of 100 to 180 mg/dL and 1.89 ± 0.80 at the glycemic range of 180 to 300 mg/dL. We calculated a flux control coefficient, C^J_{Direct}, for the direct pathway by GCK yielded 0.43 at the glycemic range of 100 to 180 mg/dL and 0.67 at the glycemic range of 180 to 300 mg/dL. Similarly, the flux control coefficients for the direct pathway by GCK were 0.39 in HFD-fed rats and 0.57 in portal delivery rats at the glycemic range of 100 to 180 mg/dL and 0.66 in HFD-fed rats and 0.78 in portal delivery rats at the glycemic range of 180 to 300 mg/dL. The flux control coefficient of GSase was found to be ~0 so that the remaining flux control for glycogen synthesis was via the indirect pathway $C^J_{Indirect}$.

GCK Antisense Oligonucleotide Treatment for GCK-Specific Control Coefficient. To independently assess the control coefficient of GCK for hepatic glycogen synthesis, we studied rats treated with an antisense oligonucleotide (ASO) against GCK. Control rats received an ASO without homology to any known gene product. Body weight during GCK ASO treatment, and plasma aspartate transaminase (AST) and alanine transaminase (ALT) activity after treatment, were similar between groups (*SI Appendix*, Fig. S5 *A* and *B*). The GCK ASO achieved hepatic GCK knockdown of ~80% at the messenger RNA (mRNA) level and ~60% at the protein level (*SI Appendix*, Fig. S5 *C* and *D*). Hyperinsulinemic–hyperglycemic clamps were performed with target glycemia of ~180 mg/dL (*SI Appendix*, Fig. S5E). Glucose infusion rates were similar between groups (*SI Appendix*, Fig. S5F). After the clamp, hepatic glycogen concentration was similar between groups (*SI Appendix*, Fig. S5G). However, the hepatic glycogen synthetic rate via the direct pathway was decreased by 37% in the GCK ASO-treated group compared with the control ASO-treated group (Fig. 4). The calculated flux control coefficient for GCK
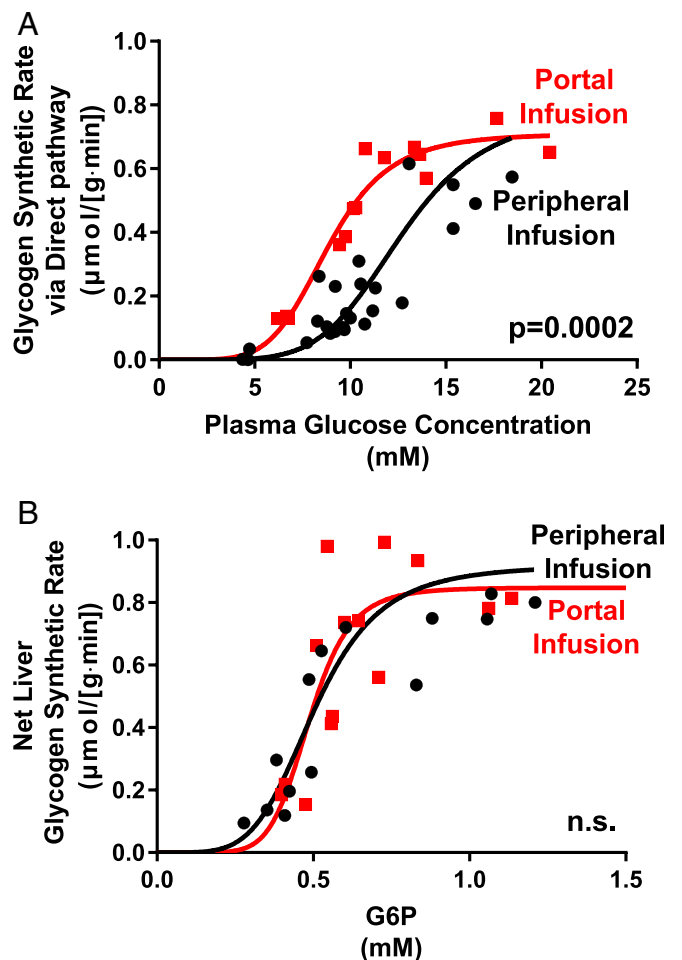
Fig. 3. The relationship between plasma glucose and direct pathway synthesis is altered while net glycogen synthesis vs. hepatic G6P content is unchanged by portal delivery of glucose. (*A*) Under hyperinsulinemic conditions (4 mU/kg·min), direct pathway glycogen synthetic rate plotted against plasma glucose concentration. Black circles: glucose infusion through peripheral vein; red squares: glucose infusion through portal vein. (*B*) Under hyperinsulinemic conditions (4 mU/kg·min), net hepatic glycogen synthesis plotted against hepatic G6P content. Black circles: glucose infusion through peripheral vein; red squares: glucose infusion through portal vein. Data fit to a sigmoidal model. n.s., not significant.

Nozaki et al.

Table 3. Calculated values of control coefficients for direct pathway, indirect pathway, and GSase for flux of glucose through glycogen synthesis

	C^J_{Direct}	$C^J_{Indirect}$	C^J_{GSase}	$R^{Jdirect}_{Glucose}$	$R^{Jindirect}_{Glucose}$	$R^{JGSase}_{Glucose}$	$\varepsilon^{Direct}_{G6P}$	$\varepsilon^{Indirect}_{G6P}$	$\varepsilon^{GSase}_{G6P}$
	Plasma glucose 100 to 180 mg/dL								
Control	0.43	0.57	~0	2.52	1.75	2.08	~0	~0	2.43
HFD	0.39	0.61	~0	1.79	0.68	1.11	~0	~0	3.56
Portal delivery	0.57	0.43	~0	1.73	1.89	1.89	~0	~0	2.51
	Plasma glucose 180 to 300 mg/dL								
	C^J_{Direct}	$C^J_{Indirect}$	C^J_{GSase}	$R^{Jdirect}_{Glucose}$	$R^{Jindirect}_{Glucose}$	$R^{JGSase}_{Glucose}$	$\varepsilon^{Direct}_{G6P}$	$\varepsilon^{Indirect}_{G6P}$	$\varepsilon^{GSase}_{G6P}$
Control	0.67	0.33	~0	1.89	0.73	1.51	~0	~0	1.40
HFD	0.66	0.35	~0	2.04	1.07	1.71	~0	~0	1.90
Portal delivery	0.78	0.22	~0	1.24	—	0.77	~0	~0	0.84

in direct pathway glycogen synthesis was 0.48, consistent with the data obtained by varying glycemia. These data support the conclusion that GCK is the primary rate-controlling factor for insulin-stimulated liver glycogen synthesis via the direct pathway.

Contributions of GCK Kinetics and GCK Activation to Responsivity to Glucose. With additional modeling, GCK activation (as by shuttling from the nucleus to the cytosol) can be separated from the intrinsic catalytic properties of GCK. Thus, to separate the contributions of GCK enzymatic kinetics from GCK activation, we performed additional MCA analysis and calculated elasticities associated with the GCK enzymatic catalysis and associated with GCK activation in all three models (Table 4). The elasticities of GCK velocity to blood glucose were 0.65, 0.65, and 0.67 in control, HFD-fed, and portal delivery rats, respectively, while the elasticities of GCK activation were 5.25, 3.95, and 2.33, respectively, at the glycemic range of 100 to 180 mg/dL. The same analysis at the glycemic range of 180 to 300 mg/dL similarly revealed high elasticities for GCK activation (Table 4). These results suggest that GCK activation more effectively contributes to GCK responsivity to glucose than GCK kinetics.

Mechanism of Activation of GCK as Rate-Controlling Step. We examined GCK mRNA and protein expression levels. GCK mRNA displayed strong up-regulation by hyperinsulinemia and was unaffected by glycemia. A similar degree of up-regulation of GCK mRNA by insulin was observed in control, HFD, and portal delivery groups (*SI Appendix*, Fig. S6 *A* and *B*).

Next, we measured liver GCK protein abundance in cytoplasmic and nuclear extracts. The cytoplasmic/nuclear ratio was significantly increased in a plasma glucose-dependent manner under hyperinsulinemic conditions (Fig. 5*A*). Interestingly, the cytoplasmic/nuclear ratio was significantly decreased in the HFD group and significantly increased in the portal delivery group compared with the RC-fed controls under conditions of hyperinsulinemia at the plasma glucose concentration 180 mg/dL (Fig. 5*B*). These results suggest that lipid-induced hepatic insulin resistance impairs GCK translocation from nucleus to cytoplasm and that portal glucose delivery promotes GCK translocation under hyperinsulinemic, hyperglycemic conditions.

Discussion

Glycogen is a multibranched polysaccharide of glucose that is stored primarily in the liver and muscle and serves as a readily mobilizable source of energy. Liver glycogen plays a crucial role in maintaining blood glucose homeostasis. Stimulation of liver glycogen synthesis is a major direct effect of insulin on the hepatocyte (1, 2) and its disruption results in postprandial hyperglycemia. The control of glycogen synthesis involves multiple insulin-regulated enzymes, and these activities coordinately change with insulin. In addition, both insulin and glucose regulate hepatic glycogen

metabolism, making assessment of their cellular effects and dose–response characteristics in vivo difficult because of the integrated nature of metabolism. As a result, the major mechanism for insulin control of glycogen synthetic flux in vivo is uncertain.

In this study, we sought first to identify the rate-controlling step in insulin-stimulated hepatic glycogen synthesis, second to investigate whether lipid-induced hepatic insulin resistance or portal vein glucose delivery affect this step, and third to determine by what mechanism rate control is exerted.

MCA analysis of the glucose dependence of the direct and indirect pathway of glycogen synthesis and G6P concentration as a function of plasma glucose concentrations revealed that GCK is a major site of rate control for insulin-stimulated hepatic glycogen synthesis. This was confirmed in studies using a GCK-specific ASO to decrease GCK expression selectively in liver. The flux control coefficient of GCK increased from 0.43, at plasma glucose concentrations of ~180 mg/dL, to 0.67, at plasma glucose concentrations of ~300 mg/dL. In contrast, GSase, which has been suggested to be a major site of rate control for hepatic glycogen synthesis (16) or to share control of hepatic glycogen synthesis with GCK (17), was found to have a comparatively low flux control coefficient and a relatively high elasticity to glucose, indicative of minimal control by GSase over hepatic glycogen synthetic rates. GSase, which is strongly regulated by allosteric effectors such as G6P, may maintain G6P homeostasis rather than controlling total glycogen synthetic flux. Taken together these results are consistent with prior studies in isolated hepatocytes
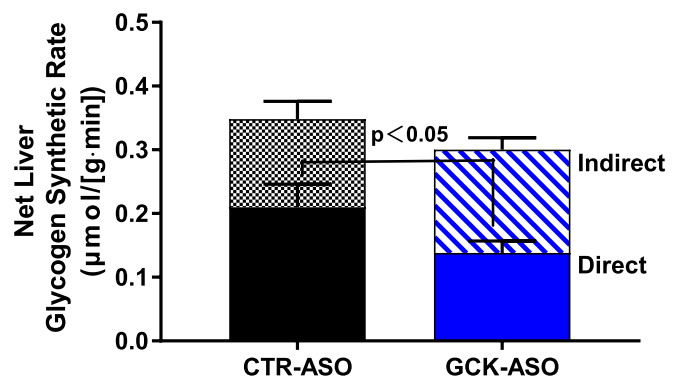
Fig. 4. GCK ASO treatment attenuates glycogen synthesis by the direct pathway. Rats received control (black bars) or GCK ASO (blue bars) and were subjected to hyperinsulinemic–hyperglycemic clamp studies (4 mU/kg·min insulin infusion rate; variable dextrose infusion targeting 180 mg/dL plasma glucose concentration). Net hepatic glycogen synthetic rates (whole bars) presented as sum of direct pathway (solid segments) and indirect pathway (patterned segments). Comparison of direct hepatic glycogen synthetic rates was statistically significant. Data are the mean ± SEM of n = 7 to 9 per group.

Nozaki et al.

www.manaraa.com

Table 4. Contributions of GCK kinetics and GKRP to responsivity to glucose: Elasticities of GCK kinetics and GKRP

	Plasma glucose 100 to 180 mg/dL		Plasma glucose 180 to 300 mg/dL	
	$\varepsilon^{GCK}_{Glucose}$(GCK)	$\varepsilon^{GCK}_{Glucose}$(GKRP)	$\varepsilon^{GCK}_{Glucose}$(GCK)	$\varepsilon^{GCK}_{Glucose}$(GKRP)
Control	0.65	5.25	0.61	2.19
HFD	0.65	3.95	0.60	2.50
Portal delivery	0.67	2.33	0.62	0.97

(18, 19) and suggest that varying the activity of the GCK step alone will change the flux in hepatic glycogen synthetic pathway more at higher plasma glucose concentrations.

Lipid-induced hepatic insulin resistance reduced hepatic glycogen synthesis via the direct pathway. The short-term (3-d) HFD model employed results in hepatic steatosis and hepatic insulin resistance without the additional confounding effects of obesity, peripheral insulin resistance, and inflammation (12). In this setting, the direct pathway flux control coefficient for GCK, and the sigmoidal dose–response relationship between hepatic G6P and hepatic glycogen synthetic rate, were both unchanged in the HFD group compared with the RC-fed controls. These results suggest that GCK is rate-controlling for hepatic glycogen synthesis in both insulin-sensitive RC-fed rats and insulin-resistant HFD-fed rats. While these experiments do not pinpoint the mechanism by which lipid-induced hepatic insulin resistance (i.e., diacylglycerol–protein kinase Cε–INSR axis) impairs insulin-stimulated hepatic glycogen synthesis (1), they do indicate that the defect in insulin-mediated hepatic glycogen synthesis is not a consequence of altered GSase phosphorylation, and instead is most likely proximal to glucose phosphorylation.

We also observed that portal vein glucose delivery augmented hepatic glycogen synthesis under conditions of hyperinsulinemia and hyperglycemia. To assess only the influence of the route of glucose administration on hepatic glycogen repletion, the portal glucose delivery group received glucose through the hepatic portal vein at a glucose infusion rate matched to the control, peripherally infused rats; insulin was delivered systemically by a carotid catheter placed at the tip of the aortic arch in both groups. Interestingly, portal glucose delivery increased the direct pathway flux control coefficient for GCK compared to controls. However, as observed in the HFD cohort, the sigmoidal relationship between G6P concentration and glycogen synthetic rate was similar between the portal delivery group and controls. We interpret this finding to indicate that the "portal factor" acts at a level proximal to G6P production. The identity of the portal factor remains ambiguous, with possible contributors including higher portal vein glycemia, zonation effects, neural involvement, and/or other mechanisms. Moreover, it is notable that the maximal velocity of hepatic glycogen synthesis during hyperinsulinemia was identical between the portal infusion and peripheral infusion groups. This saturation behavior is consistent with a model wherein GCK translocation controls glycogen synthesis: At a certain point, GCK translocation is complete, and GCK catalysis reaches its maximal velocity.

Remarkably, while there were significant differences in reactivity of hepatic glycogen synthesis to plasma glucose concentrations between the HFD-fed model or the portal infusion model and the control, these three regression lines superimposed in correlation between hepatic glycogen synthesis and liver G6P concentrations. Thus, the product catalyzed by GCK, liver G6P, was the best predictor of liver glycogen synthetic rate in all three models. Taken together these data suggest that the main mechanism by which liver insulin resistance reduces the rate of glycogen synthesis is via a defect in the activation of hepatic GCK, and that alterations in GCK activity can also fully explain the portal factor.

One fundamental finding of this study was that hyperglycemia and hyperinsulinemia are each necessary but insufficient for net hepatic glycogen synthesis, which is consistent with prior studies
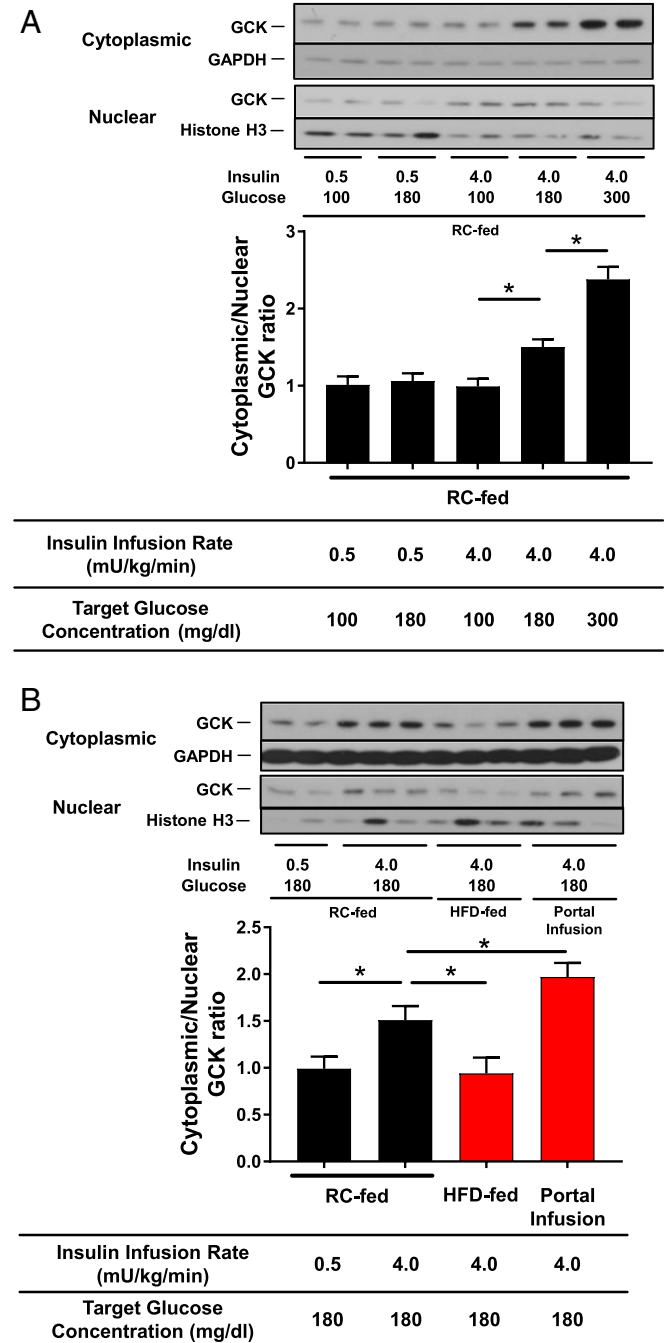
Fig. 5. Cytoplasmic translocation of GCK decreases with insulin resistance and increases with portal glucose infusion. Rats subject to somatostatin clamps (conditions specified in figure). Immunoblots presented for nuclear and cytoplasmic compartments. GCK content compared with histone H3 in the nuclear compartment and with GAPDH in the cytoplasmic compartment. (A) GCK translocation as a function of insulin infusion and plasma glucose target in RC-fed, peripherally infused rats and (B) GCK translocation comparing RC-fed, peripherally infused control rats with HFD-fed, peripherally infused rats and with RC-fed, portally infused rats. Data are the mean ± SEM of n = 6 to 8 per group. *P < 0.05 by unpaired Student's t test.

Nozaki et al.

PHYSIOLOGY
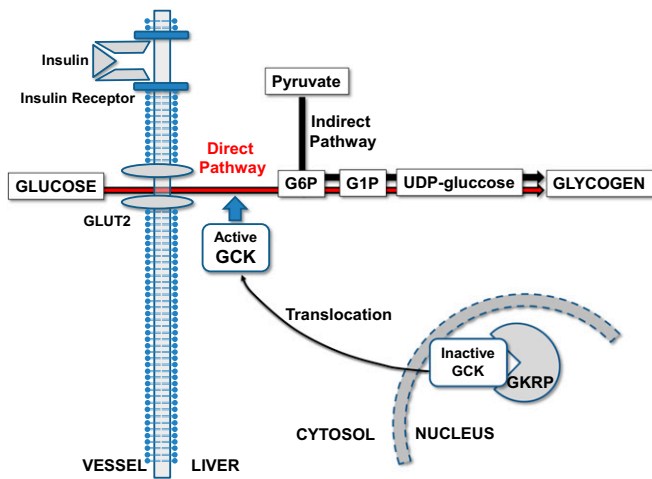
Fig. 6. Schema. GCK translocation is rate-controlling for insulin-stimulated liver glycogen synthesis through acting as the initial step of glucose phosphorylation.

in humans (20). In the setting of permissive hyperinsulinemia, increases in glucose flux dose-dependently increase hepatic glycogen synthetic rates. These results can help to explain several previous studies of the humoral regulation of hepatic glycogen metabolism. In the presence of hyperinsulinemia, hyperglycemia has been observed to be the primary factor driving hepatic glycogen synthesis, particularly through the direct pathway (21). In our model, insulin is a permissive factor for stimulation of hepatic glycogen synthesis: Neither physiological nor pharmacological levels of insulin can stimulate net hepatic glycogen synthesis in the absence of hyperglycemia. Furthermore, in humans, hyperinsulinemia is required for stimulation of hepatic GSase flux, and hyperglycemia is required for the suppression of hepatic glycogenolysis; these paired roles of insulin and glucose were interpreted as important to prevent futile hepatic glycogen cycling (1, 20). Similarly, the paired requirements for insulin and glucose for the activation of glycogen synthesis ensure that this process occurs only under optimal postprandial conditions and not under stress conditions when hyperglycemia may be present in the absence of hyperinsulinemia. Furthermore, the steep sigmoidal kinetic behavior described here, wherein the direct pathway accelerates at ~7 mM plasma glucose concentrations, is optimal to support a role for hepatic glycogen accretion in maintaining normal glucose homeostasis.

The last question addressed by this study is by what mechanism GCK is regulated in the liver. GKRP is a key player in the regulation of hepatic GCK. GKRP forms a complex with GCK, inhibiting GCK while also maintaining a stable pool of GCK available when needed. Prior in vitro studies have shown that the effect of GKRP on glycogen synthetic flux is nearly perfectly reciprocal to the effect of GCK on this flux (5, 22, 23). GCK gene expression is induced by insulin (24) and potentially reduced by G6P but is not directly affected by high glucose. G6P produced by GCK has a greater effect on GSase (25). In contrast, GKRP mRNA is induced by high glucose concentrations (26), but apparently not by insulin (27). Furthermore, GCK protein expression is regulated and stabilized by GKRP protein at the posttranscriptional level (5, 27). Two mechanisms are involved in the regulation of GCK activity: transcriptional mechanisms which account for chronic changes in protein expression (28) and translocation from the nucleus to the cytoplasm which accounts for the acute changes in postprandial glucose uptake (19, 29). In our study, hyperinsulinemia induced GCK mRNA expression ~25-fold, and

under conditions of hyperinsulinemia, hyperglycemia induced GCK translocation from nucleus to cytoplasm in the physiological state. In our short-duration clamp experiments, GCK activity is likely primarily controlled by protein translocation from the cytoplasm to the nucleus. This was supported by the result of our MCA showing that contributions of GCK activation to responsivity to glucose were higher compared with GCK kinetics. Studies using cultured hepatocytes have shown that glucose per se is a potent stimulator of GCK translocation, whereas the results regarding the effects of insulin are controversial (30–33). Our results suggest that both insulin and glucose are essential for GCK translocation in vivo; at basal insulin concentrations, hyperglycemia did not promote GCK translocation. Of note, the mechanism whereby insulin permits translocation to occur is not clear. Interestingly, GCK translocation was reduced in lipid-induced liver insulin resistance and promoted when glucose was infused intraportally compared with RC-fed rats infused with glucose peripherally, while no difference was observed in GCK mRNA expression levels. Based on these results, and our findings that both the defect in glycogen synthesis in hepatic lipid-induced insulin resistance and the increment in glycogen synthesis seen with portal glucose infusion are both explained by GCK flux, we suggest that regulation of GCK translocation is the key to understanding regulation of hepatic glycogen synthesis (Fig. 6). These results are consistent with the findings of Wan et al. (34) showing that GSK3 activity is not necessary for insulin-stimulated hepatic glycogen synthesis.

Consistent with these results, patients with maturity-onset diabetes mellitus of the young type 2 (MODY2), a disorder caused by loss-of-function mutations in GCK, demonstrate reduced postprandial hepatic glycogen synthesis (35). Most patients with MODY2 have heterozygous loss of function mutations and exhibit a 30 to 60% decrease in postprandial glycogen synthesis. Building on basic studies demonstrating dysfunction of GCK-mediated glucose sensing in pancreas and liver in the progression of T2D and nonalcoholic fatty liver disease, GCK activators have been investigated for therapeutic utility in humans. GCK activators were highly effective in phase 1 trials in patients with T2D; however, subsequent phase 2 trials revealed problems including hyperlipidemia, hypertension, and loss of drug efficacy within several months (36–39). Recently, genome-wide association studies indicating that variants in the gene encoding GKRP (which is expressed only in liver) protect against T2DM (40) provide insight into the possible efficacy and safety of GKRP targeting in humans (4).

There are several potential limitations on the application of MCA in vivo, of which we address the two most significant for our study. In principle, the control coefficients and elasticities are derivatives, and therefore the calculations from finite deltas in glucose concentration and glycogen synthesis flux represent average values. However, by obtaining a range of glucose concentrations we were able to show that both the responsivity of GCK to glucose and the elasticity of GSase are sigmoidal functions of glucose and G6P, respectively. The curve fits of the data clearly demonstrate that the average control coefficients calculated from the 5 to 10 mM and the 10 to 20 mM increments in glucose apply throughout these ranges. A second potential limitation would arise if an enzyme within the system is altered by an effector or signaling protein not included in the model. For GCK it is well established that the major factor influencing its activity is translocation, and in accord with in vitro studies we directly showed that there is minimal G6P feedback. For GSase we were able to show through plotting G6P vs. glycogen synthesis flux that under all conditions the kinetics with respect to G6P were unchanged. Therefore, both the phosphorylation state of GSase and the concentration of any other potential allosteric effectors besides G6P had to be effectively the same in all conditions and groups studies (13).

www.manaraa.com

In conclusion, these findings demonstrate that GCK catalyzes the rate-controlling step in insulin-stimulated hepatic glycogen synthesis. Physiologically relevant perturbations in insulin-stimulated hepatic glycogen synthesis, such as the reduction seen in lipid-induced hepatic insulin resistance and the augmentation due to portal delivery of glucose, can be essentially entirely explained by differences in G6P production downstream of alterations in GCK translocation.

Methods

Animal Procedures. Male Sprague-Dawley rats (weighing 260 to 280 g; Charles River Laboratories) were given at least 1 wk to acclimate and housed at the animal care facility at the Yale University Animal Research Center and maintained under controlled temperature (22 ± 2 °C) on a 12-h:12-h light/dark cycle and with free access to food and water. Rats were maintained on a standard RC diet (Harlan Teklad 21085: 58% carbohydrate, 18% fat, 24% protein calories); rats in HFD groups were placed on a HFD (Dyets 112245: 26% carbohydrate, 59% fat, 15% protein calories; Dyets Inc.) for 3 d before infusions. Rats underwent the placement of jugular venous catheters for blood sampling and carotid artery and portal vein catheters for infusion ~10 d before the terminal studies. They recovered their presurgical weights by 5 to 7 d after the operation. All infusions were done after 14- to 16-h overnight fast.

Somatostatin Pancreatic Clamp Studies. To examine liver glycogen synthesis at several plasma insulin and glucose concentrations, we employed somatostatin pancreatic clamps in rats. We studied five permutations of plasma insulin and glucose target levels: group 1, low insulin/euglycemia; group 2, low insulin/hyperglycemia; group 3, high insulin/euglycemia; group 4, high insulin/hyperglycemia; and group 5, high insulin/marked hyperglycemia. These five groups were studied in each of the following three models: RC-fed rats (control), insulin-resistant rats fed a HFD for 3 d (HFD), and RC-fed rats in which glucose was infused through the portal vein at rates matched to those used in the control cohort (portal delivery). For HFD groups, we studied another permutation of high insulin and marked hyperglycemia (400 mg/dL). Somatostatin (1:1 mix of somatostatin-14 and somatostatin-28 in normal saline; Bachem) was infused at 4 μg/(kg·min) to suppress endogenous insulin and glucagon. Insulin was infused at rates of 0.5 (basal replacement) or 4.0 (hyperinsulinemia) mU/(kg·min), as previously described (41). Glucose including [$^{13}C_6$] glucose as a tracer was infused to maintain three target glucose concentrations of euglycemia (100 mg/dL), hyperglycemia (180 mg/dL), or marked hyperglycemia (300 or 400 mg/dL), respectively. Blood samples were collected in the basal state and throughout the experiment. Clamp studies lasted 90 min to avert somatostatin breakthrough. After 90 min, the animals were anesthetized with pentobarbital and their livers were removed and freeze-clamped in liquid nitrogen.

Isotope and Infusate Preparations. Human insulin (Novo Nordisk) was diluted in saline with a small amount of bovine serum albumin (BSA) (10 μL of 10% [wt/vol] BSA in 10 mL saline) to prevent adhesion to tubing. Forty percent (wt/vol) glucose was prepared with 20% (wt/vol), [$^{13}C_6$] glucose (Cambridge Isotope Labs) and 20% (wt/vol) dextrose in water.

Liver Glycogen Synthesis. Total liver glycogen and pathway-specific glycogen synthetic rates were measured after amyloglucosidase digestion of tissue extracts as previously described (10, 42).

Liver Glucose Metabolites and Lipid Measurements. Liver G6P concentrations were measured using an enzymatic assay kit according to the manufacturer's instructions (G6P Assay Kit MAK014; Sigma-Aldrich). Liver UDP-glucose was measured by liquid chromatography MS/MS. Liver triglycerides were extracted by the method of Bligh and Dyer (43) and measured using a colorimetric assay (Sekisui).

MCA of Hepatic Glycogen Synthesis. MCA was used to quantitatively determine the relative roles of the direct pathway (via GCK activity), GSase, and the indirect pathway in controlling the rate of glycogen synthesis at different levels of glucose using an approach similar to what we have previously used in muscle (44) but extended to include the indirect pathway of glycogen synthesis. In MCA flux control coefficients are quantitative measures of the control an enzyme exerts on the flux of a metabolic

pathway (44). The mathematical expression used to define flux control is given in Eq. **1**:

$$C_i^J = \frac{\frac{\delta J}{J}}{\frac{\delta E_i}{E_i}},$$ **[1]**

where C is the control coefficients of enzyme i over pathway j, J is a pathway flux, and E_i is the concentration of enzyme. The coefficient is a measure of the fractional change in pathway flux as a function of a fractional change in the enzyme activity.

The relationship between the control coefficients of the enzymes in a pathway has been shown to be determined by the elasticity theorem in which elasticity is defined as the fractional change of an enzyme rate in response to a fractional change of one of its substrates, products, or allosteric modulators (7, 45). The elasticity coefficient of an enzyme i to a substrate S is defined by

$$\varepsilon_S^i = \frac{\delta V_i / V_i}{\delta S / S},$$ **[2]**

where V_i is the enzyme velocity under the in vivo condition that is determined by E_i and concentration of substrate and allosteric effectors S.

In order to determine the flux control coefficients we used two different approaches. In the first approach we measured G6P concentration and the pathways of glycogen synthesis at three levels of glucose. These measurements were then used to calculate the control coefficients as described below. In the second approach we directly measured the control coefficient of the direct pathway by measuring the reduction in the direct pathway flux when the activity of GCK was knocked down using an ASO approach.

Model of Hepatic Glycogen Synthesis. For each of the fluxes entering or exiting the G6P pool there are two or more enzymes involved. However, it has been shown that each separate branch can be treated in MCA as single equivalent enzymes. As described in *Discussion* the major enzyme that controls the direct pathway is GCK and the major enzyme that controls the flux of glycogen synthesis from G6P is GSase.
Summation theorem. The relationships between control coefficients are described in four equations derived from theorems in MCA. The first equation is derived from the summation theorem, which states that the sum of all control coefficients in a system is equal to 1 (Eq. 3) (7):

$$C_{GCK}^J + C_{GSase}^J + C_{Indirect}^J = 1.$$ **[3]**

Elasticity theorem. The second relationship derives from elasticity theorem, which states that if enzymes in a pathway share a common allosteric effector/substrate (e.g., G6P in the glycogen synthesis pathway) the control coefficients are inversely related to the elasticities. As a consequence enzymes that are highly sensitive to an effector exert little flux control. For the glycogen synthesis pathway the elasticity relationship to G6P is given in Eq. 4:

$$C_{GCK}^J * \varepsilon_{G6P}^{GCK} + C_{GSase}^J * \varepsilon_{G6P}^{GSase} + C_{Indirect}^J * \varepsilon_{G6P}^{Indirect} = 0.$$ **[4]**

An additional relationship can be determined if a branch point exists where a pathway splits into two or more other pathways (46). In the case of the hepatic glycogen synthesis pathway there is a branch point at G6P. The branch point equation describing the system is given in Eq. 5:

$$C_{GCK}^J / J_{GCK} + C_{GSase}^J / J_{GSase} - C_{Indirect}^J / J_{Indirect} = 0.$$ **[5]**

Responsivity theorem. The final relationship used was derived from the responsivity theorem of MCA (45). This theorem relates the change in pathway flux when the initial substrate (in the case of the direct pathway plasma glucose) is changed to the control coefficient and elasticity of the first enzyme in the system as described in Eq. 6:

$$R_{Gi}^J = \varepsilon_{Gi}^{GCK} * C_{GCK}^J.$$ **[6]**

Determination of System Elasticities to G6P.
Elasticity of GSase. The elasticity to G6P for GSase was calculated using the following formula for the increments in glucose level between 100 and 180 mg/dL and 180 to 300 mg/dL:

$$\varepsilon_{G6P}^{GSase} = \frac{\delta V_{GSase} / V_{GSase}}{\delta G6P / G6P}.$$ **[7]**

The value of V_{GSase} was determined from the measured glycogen synthesis flux at the two glucose levels. The value of V_{GSase} and *G6P* used in the

Nozaki et al.

PHYSIOLOGY

www.manaraa.com

denominator was the lower of the two values for each increment (100 and 180 mg/dL) to provide a better approximation of the elasticity and control coefficients at the lower concentration.

In addition to calculation of the elasticity based upon the measured increments we also performed a second analysis in which we calculated the elasticity as a continuous function of G6P concentration.

Elasticity of indirect pathway. The elasticity to G6P for the indirect pathway was calculated using the following formula for the increments in glucose level between 100 and 180 mg/dL and 180 to 300 mg/dL:

$$\varepsilon_{G6P}^{Indirect} = \frac{\delta \text{Vindirect}/Vindirect}{\delta G6P/G6P}. \quad [8]$$

The value of Vindirect was determined from the measured glycogen synthesis flux at the two glucose levels. The value of *Vindirect* and *G6P* used in the denominator was the lower of the two values for each increment (100 and 180 mg/dL) to provide a better approximation of the elasticity and control coefficients at the lower concentration.

The sign of the elasticity of the indirect pathway is negative since G6P is an end product and does not allosterically stimulate any of the enzymes in the indirect pathway. When a positive elasticity was measured, most likely due to a shunting of a greater fraction of the indirect flux into glycogen synthesis at higher glucose levels due to the direct pathway supplying the glucose needs of the pentose phosphate and other G6P-dependent pathways, the value of $\varepsilon_{G6P}^{Indirect}$ was set to 0.

Elasticity of the direct pathway (GCK) to G6P. Determining the elasticity of the direct pathway to G6P is complicated by changes in both glucose and G6P as well as glucose-dependent activation of GCK. However, the elasticity as a function of G6P can be calculated using the following general expression (44):

$$\varepsilon_{S2}^{E1} = \frac{-p}{1-p} - Q_2, \quad [9]$$

where p is the disequilibrium ratio which is the ratio of concentrations of the chemical reactants divided by the equilibrium constant for the reaction. The term Q_2 is defined as

$$Q_2 = \frac{S2}{M2} \cdot \frac{1}{\left(1 + \frac{S1}{M1} + \frac{S2}{M2} + \frac{Sa}{Ma} + \dots\right)}, \quad [10]$$

where *M1* is the Michaelis constant (K_M) for intracellular glucose, *S1* is the concentration of intracellular glucose, *M2* is the inhibition constant (K_i) for G6P, and *S2* is the concentration of G6P. All other terms are set to 0.

The GCK reaction is far from equilibrium so that p ∼ 0. For *Q2* based on kinetic studies *M2* is very high so that at in vivo concentrations of G6P *S2/M2* is also ∼ 0. Therefore, for the flux control coefficient calculations we approximated $\varepsilon_{G6P}^{direct} \sim 0$.

Contributions of GCK Kinetics and GCK Activation to the Responsivity of the Direct Pathway to Glucose Concentration. The flux through the direct pathway as a function of plasma glucose depends upon both the kinetic properties of GT, GCK, and the number of active GCK molecules. In order to separate the relative contributions to the direct pathway we measured the responsivity of the direct pathway flux to plasma glucose concentration (Eq. **13**). The responsivity can be related to the elasticity of the direct pathway to the concentration of plasma glucose and the combined control coefficient of GT and GCK using the responsivity theorem (Eq. **11**):

$$R_{Go}^{Jdirect} = \varepsilon_{Go}^{GCK/GT} * C_{GCK/GT}^{Jdirect}. \quad [11]$$

Because of the low control coefficient of GSase the combined control coefficient of GCK/GT of the direct pathway is ∼1. Furthermore, it was found that intracellular glucose concentrations were approximately equal to plasma levels, indicating no control exerted by GT. Setting *$C_{GCK/GT}^{Jdirect}$ equal to 1 and only considering the contribution to the responsivity of the system from GCK simplified Eq. **11** to

$$R_{Go}^{Jdirect} = \varepsilon_{Go}^{GCK}. \quad [12]$$

For GCK the dependence of flux on glucose concentration is due to two factors: 1) the Michaelis–Menten kinetics of GCK and 2) the number of active GCK molecules increasing as a function of intracellular glucose due to GKRP and other factors. The relations between the elasticity of GCK at a constant total activity level and the contribution to the total elasticity from the GKRP-

mediated glucose dependence of the total activity of GCK are made explicit in the equation below (44) (where *Go* is considered to be ∼ *Gi*):

$$\varepsilon_{Go}^{GCK} = \varepsilon_{Go}^{GCK}(GCK) + \varepsilon_{Go}^{GCK}(GCKact). \quad [13]$$

The first term in Eq. **12** is the elasticity of a constant concentration of active GCK molecules with respect to intracellular glucose. The second term is the elasticity of GCK with respect to intracellular glucose due to the increase in active GCK molecules).

Eq. **13** is derived by expressing the enzyme activity of GCK as a function of intracellular glucose as the product of two terms:

$$V_{GCK}(Go) = GCKact(Go) * V_{GCK}(Go). \quad [14]$$

With GCKact (Go) being the total activity of GCK (proportional to the number of active GCK molecules per volume of tissue and V_{max} of a single enzyme) and V_{GCK}(Go) being the kinetic description with respect to glucose concentration of a single active GCK molecule normalized to V_{max} =1. Taking the derivative of Eq. **14** with respect to Go and multiplying by Go/V_{GCK}(Go) yields Eq. **13**.

GCK has Michaelis–Menten kinetics and the catalyzed reaction is far from equilibrium due to the consumption of adenosine 5′-triphosphate. In addition, there is no feedback inhibition from G6P at physiological levels. The elasticity is then given by

$$\varepsilon_{Go}^{GCK}(GCK) = 1 - \frac{Go/K_M}{1 + Go/K_M}. \quad [15]$$

Substituting in the expression for $\varepsilon_{Go}^{GCK}(GCK)$ into Eq. **13** gives

$$\varepsilon_{Go}^{GCK}(GCKact) = \varepsilon_{Go}^{GCK} - \left(1 - \frac{Go/K_M}{1 + Go/K_M}\right). \quad [16]$$

The value of the two components of $\varepsilon_{Go}^{GCK}(GCKact)$ are seen to depend upon the K_M of GCK.

The minimum value of $\varepsilon_{Go}^{GCK}(GCKact)$ takes place when $Go/K_M \ll 1$:

$$\varepsilon_{Go}^{GCK}(GCKact)_{min} = \varepsilon_{Go}^{GCK} - 1. \quad [17]$$

We calculated $\varepsilon_{Go}^{GCK}(GCK) and \varepsilon_{Go}^{GCK}(GCKact)$ using Eq. **12** with the measured responsivities and Eq. **15** for K_M values of 5 mM, 10 mM, 15 mM, and 20 mM, respectively, which covers the full range of reported K_M values in the literature.

GCK ASO Study. Based on the high hepatic glucose level it was concluded that the large majority of the control of the direct pathway was due to GCK. To test this conclusion we independently measured the control coefficient of GCK directly by varying its activity using an ASO approach.

Rat GCK and control (CTR) ASOs were designed and produced as previously described (47). The sequence 5-TCCGCCATTTTCTGTAGTTG-3 (ISIS-793987) was selected for rat GCK and the sequence 5-CCTTCCCTGAAGGTTCCTCC-3 (ISIS-141923) was selected as the CTR ASO. ASOs were injected intraperitoneally at a dose of 50 mg/kg weekly for 2 wk.

Rats underwent the placement of jugular venous catheters for blood sampling and carotid artery catheters for infusion ∼10 d before the terminal studies. They recovered their presurgical weights by 5 to 7 d after the operation. The somatostatin pancreatic clamp studies were then performed. The [$^{13}C_6$] glucose was infused via the peripheral artery to maintain hyperglycemia (∼180 mg/dL) and insulin was infused at 4 mU/(kg·min) via a peripheral artery.

The GCK-specific control coefficient in liver was calculated as

$$C_{GCK}^J = \frac{V_{syn\,(CTR-ASO)} - V_{syn\,(GCK-ASO)}/V_{syn\,(CTR-ASO)}}{1 - Fraction_{active}/1}.$$

Kinetic Parameter Two-State Sigmoidal Curve Fits. Glycogen synthetic rates were fit to the model of Palm et al. (13), a sigmoidal two-state (active/inactive) kinetic model, according to the following equation:

$$V_{GCK([G6P])} = \frac{([G6P]/K_a)^H}{1 + ([G6P]/K_a)^H} V_{max}. \quad [18]$$

This model has been shown to accurately fit the kinetics of GSase in solution and in vivo. The parameters optimized to obtain the best least squares fit to the data were the Hill coefficient *H*, maximum glycogen synthesis rate V_{max}, and K_a (concentration of the independent variable that yields half-maximal

velocity). In order to determine the distribution of the kinetic constants, we performed a Monte Carlo simulation in which we added random noise at a level determined from the deviation of the data from the best-fit values of the H, K_a, and V_{max}. The noise simulation and fitting were repeated 10,000 times to obtain histograms of the distributions of values and their relative probabilities. We then calculated the P value for difference between the constants based on the overlap of the distributions in the two conditions.

Biochemical Analysis. Plasma rat C-peptide and infused human insulin were measured using enzyme-linked immunosorbent assay (ELISA) kits (ALPCO rat C-peptide ELISA kit and Mercodia Insulin ELISA, respectively).

Western Blotting. For whole-cell lysate preparation, 100 mg liver was homogenized in 1 mL ice-cold homogenation buffer (20 mM Tris·HCl, pH 7.4, 5 mM EDTA, 0.25 mM EGTA, 10 mM $Na_4P_2O_7$, 1% Nonidet P-40, 1 mM PMSF, and 10 μg/mL aprotinin) and the protein concentration was determined by the Bradford method (Bio-Rad). Akt and phosphorylated Akt were detected with whole-cell lysates. Akt and phosphorylated Akt (Ser473) antibodies were from Cell Signaling Technology, Inc.

GCK Translocation Assay. Cytosolic and nuclear extractions in liver were prepared using NE-PER Nuclear and Cytoplasmic Extraction Reagents (Thermo Fisher Scientific) (48). GCK was detected in both cytoplasmic and nuclear proteins. The GCK antibody was a kind gift of M. Magnuson, Vanderbilt University School of Medicine, Nashville, TN. GCK translocation was expressed as the ratio of cytoplasmic band intensity to nuclear band intensity. Cytoplasmic band density was normalized to glyceraldehyde-3-phosphate dehydrogenase (GAPDH) band intensity (Cell Signaling Technology, Inc.) and nuclear band intensity was corrected by histone H3 band intensity (Abcam Inc.).

Quantitative Real-Time PCR. Total RNA was isolated from ~15 mg liver using an RNeasy Mini Kit (Qiagen). RNA was reverse-transcribed into complementary DNA with the use of M-MuLV Reverse Transcriptase (New England

Biolabs). The abundance of transcripts was assessed by real-time PCR on an Applied Biosystems 7500 Fast Real-Time PCR System (Applied Biosystems) with a SYBR Green detection system (Stratagene). The expression data for each gene of interest were normalized for the efficiency of amplification with TATA box binding protein mRNA as the invariant control, as determined by a standard curve. PCR was carried out by using the primer 5′-agacctgggaggaaccaact and 5′- tttgtcttcacgctccactg.

Statistical Analysis. Data were compared using the Student's unpaired t test or ANOVA with the Tukey post hoc test between two groups or more than two groups, respectively. SPSS for Windows, version 22 (IBM Co.) and GraphPad Prism 7.0 software were used for all statistical analysis. Analysis of covariance were performed to compare two nonlinear regressions using GraphPad Prism 7.0 (49).

All data were expressed as mean ± SEM. P values of less than 0.05 were considered significant.

Study Approval. All experimental protocols involving animals were approved by the Institutional Animal Care and Use Committee of Yale University.

Material and Data Availability. Sources for materials used in this study are described in *Materials and Methods*. The raw data obtained for this study are presented in Dataset S1.

1. M. C. Petersen, D. F. Vatner, G. I. Shulman, Regulation of hepatic glucose metabolism in health and disease. *Nat. Rev. Endocrinol.* **13**, 572–587 (2017).
2. G. I. Shulman, B. R. Landau, Pathways of glycogen repletion. *Physiol. Rev.* **72**, 1019–1035 (1992).
3. F. M. Matschinsky, Glucokinase as glucose sensor and metabolic signal generator in pancreatic beta-cells and hepatocytes. *Diabetes* **39**, 647–652 (1990).
4. M. C. G. J. Brouwers, C. Jacobs, A. Bast, C. D. A. Stehouwer, N. C. Schaper, Modulation of glucokinase regulatory protein: A double-edged sword? *Trends Mol. Med.* **21**, 583–594 (2015).
5. J. Grimsby et al., Characterization of glucokinase regulatory protein-deficient mice. *J. Biol. Chem.* **275**, 7826–7831 (2000).
6. D. A. Fell, Metabolic control analysis: A survey of its theoretical and experimental development. *Biochem. J.* **286**, 313–330 (1992).
7. H. Kacser, J. A. Burns, The control of flux. *Symp. Soc. Exp. Biol.* **27**, 65–104 (1973).
8. J. R. Chase, D. L. Rothman, R. G. Shulman, Flux control in the rat gastrocnemius glycogen synthesis pathway by in vivo 13C/31P NMR spectroscopy. *Am. J. Physiol. Endocrinol. Metab.* **280**, E598–E607 (2001).
9. S. Aiston, L. Hampson, A. M. Gómez-Foix, J. J. Guinovart, L. Agius, Hepatic glycogen synthesis is highly sensitive to phosphorylase activity: Evidence from metabolic control analysis. *J. Biol. Chem.* **276**, 23858–23866 (2001).
10. M. C. Petersen et al., Insulin receptor Thr1160 phosphorylation mediates lipid-induced hepatic insulin resistance. *J. Clin. Invest.* **126**, 4361–4371 (2016).
11. S. Cardin et al., Portal glucose infusion increases hepatic glycogen deposition in conscious unrestrained rats. *J. Appl. Physiol.* **87**, 1470–1475 (1999).
12. V. T. Samuel et al., Mechanism of hepatic insulin resistance in non-alcoholic fatty liver disease. *J. Biol. Chem.* **279**, 32345–32353 (2004).
13. D. C. Palm, J. M. Rohwer, J. H. Hofmeyr, Regulation of glycogen synthase from mammalian skeletal muscle–A unifying view of allosteric and covalent regulation. *FEBS J.* **280**, 2–27 (2013).
14. G. C. Canavos, "A Monte Carlo investigation of experimental data requirements for fitting polynomial functions" (NASA Tech. Note D-7516, NASA, Washington, DC, 1974), p. 24.
15. G. F. Mason, K. L. Behar, D. L. Rothman, R. G. Shulman, NMR determination of intracerebral glucose concentration and transport kinetics in rat brain. *J. Cereb. Blood Flow Metab.* **12**, 448–455 (1992).
16. P. J. Roach et al., Novel aspects of the regulation of glycogen storage. *J. Basic Clin. Physiol. Pharmacol.* **9**, 139–151 (1998).
17. R. R. Gomis, J. C. Ferrer, J. J. Guinovart, Shared control of hepatic glycogen synthesis by glycogen synthase and glucokinase. *Biochem. J.* **351**, 811–816 (2000).
18. L. Härndahl, D. Schmoll, A. W. Herling, L. Agius, The role of glucose 6-phosphate in mediating the effects of glucokinase overexpression on hepatic glucose metabolism. *FEBS J.* **273**, 336–346 (2006).
19. L. Agius, Glucokinase and molecular aspects of liver glycogen metabolism. *Biochem. J.* **414**, 1–18 (2008).
20. K. F. Petersen, D. Laurent, D. L. Rothman, G. W. Cline, G. I. Shulman, Mechanism by which glucose and insulin inhibit net hepatic glycogenolysis in humans. *J. Clin. Invest.* **101**, 1203–1209 (1998).
21. G. I. Shulman, R. A. DeFronzo, L. Rossetti, Differential effect of hyperglycemia and hyperinsulinemia on pathways of hepatic glycogen repletion. *Am. J. Physiol.* **260**, E731–E735 (1991).
22. A. Raimondo, M. G. Rees, A. L. Gloyn, Glucokinase regulatory protein: Complexity at the crossroads of triglyceride and glucose metabolism. *Curr. Opin. Lipidol.* **26**, 88–95 (2015).
23. N. de la Iglesia, M. Mukhtar, J. Seoane, J. J. Guinovart, L. Agius, The role of the regulatory protein of glucokinase in the glucose sensory mechanism of the hepatocyte. *J. Biol. Chem.* **275**, 10597–10603 (2000).
24. P. B. Iynedjian, D. Jotterand, T. Nouspikel, M. Asfari, P. R. Pilot, Transcriptional induction of glucokinase gene by insulin in cultured liver cells and its repression by the glucagon-cAMP system. *J. Biol. Chem.* **264**, 21824–21829 (1989).
25. J. Seoane et al., Glucose 6-phosphate produced by glucokinase, but not hexokinase I, promotes the activation of hepatic glycogen synthase. *J. Biol. Chem.* **271**, 23756–23760 (1996).
26. L. Ma, L. N. Robinson, H. C. Towle, ChREBP*Mlx is the principal mediator of glucose-induced gene expression in the liver. *J. Biol. Chem.* **281**, 28721–28730 (2006).
27. D. Farrelly et al., Mice mutant for glucokinase regulatory protein exhibit decreased liver glucokinase: A sequestration mechanism in metabolic regulation. *Proc. Natl. Acad. Sci. U.S.A.* **96**, 14511–14516 (1999).
28. P. B. Iynedjian, Molecular physiology of mammalian glucokinase. *Cell. Mol. Life Sci.* **66**, 27–42 (2009).
29. K. S. Cullen, Z. H. Al-Oanzi, F. P. O'Harte, L. Agius, C. Arden, Glucagon induces translocation of glucokinase from the cytoplasm to the nucleus of hepatocytes by transfer between 6-phosphofructo 2-kinase/fructose 2,6-bisphosphatase-2 and the glucokinase regulatory protein. *Biochim. Biophys. Acta* **1843**, 1123–1134 (2014).
30. Y. Fujimoto, E. P. Donahue, M. Shiota, Defect in glucokinase translocation in Zucker diabetic fatty rats. *Am. J. Physiol. Endocrinol. Metab.* **287**, E414–E423 (2004).
31. L. Agius, M. Peak, Intracellular binding of glucokinase in hepatocytes and translocation by glucose, fructose and insulin. *Biochem. J.* **296**, 785–796 (1993).
32. K. S. Brown, S. S. Kalinowski, J. R. Megill, S. K. Durham, K. A. Mookhtiar, Glucokinase regulatory protein may interact with glucokinase in the hepatocyte nucleus. *Diabetes* **46**, 179–186 (1997).
33. Y. Toyoda et al., Changes in subcellular and zonal distribution of glucokinase in rat liver during postnatal development. *FEBS Lett.* **359**, 81–84 (1995).
34. M. Wan et al., A noncanonical, GSK3-independent pathway controls postprandial hepatic glycogen deposition. *Cell Metab.* **18**, 99–105 (2013).
35. G. Velho et al., Impaired hepatic glycogen synthesis in glucokinase-deficient (MODY-2) subjects. *J. Clin. Invest.* **98**, 1755–1761 (1996).
36. J. Grimsby et al., Allosteric activators of glucokinase: Potential role in diabetes therapy. *Science* **301**, 370–373 (2003).

Nozaki et al.

37. R. C. Bonadonna et al., Piragliatin (RO4389620), a novel glucokinase activator, lowers plasma glucose both in the postabsorptive state and after a glucose challenge in patients with type 2 diabetes mellitus: A mechanistic study. *J. Clin. Endocrinol. Metab.* **95**, 5028–5036 (2010).

38. G. E. Meininger et al., Effects of MK-0941, a novel glucokinase activator, on glycemic control in insulin-treated patients with type 2 diabetes. *Diabetes Care* **34**, 2560–2566 (2011).

39. F. M. Matschinsky, GKAs for diabetes therapy: Why no clinically useful drug after two decades of trying? *Trends Pharmacol. Sci.* **34**, 90–99 (2013).

40. E. K. Speliotes et al.; NASH CRN; GIANT Consortium; MAGIC Investigators; GOLD Consortium, Genome-wide association analysis identifies variants associated with nonalcoholic fatty liver disease that have distinct effects on metabolic traits. *PLoS Genet.* **7**, e1001324 (2011).

41. D. F. Vatner et al., Insulin-independent regulation of hepatic triglyceride synthesis by fatty acids. *Proc. Natl. Acad. Sci. U.S.A.* **112**, 1143–1148 (2015).

42. J. V. Passonneau, V. R. Lauderdale, A comparison of three methods of glycogen measurement in tissues. *Anal. Biochem.* **60**, 405–412 (1974).

43. E. G. Bligh, W. J. Dyer, A rapid method of total lipid extraction and purification. *Can. J. Biochem. Physiol.* **37**, 911–917 (1959).

44. R. G. Shulman, G. Bloch, D. L. Rothman, In vivo regulation of muscle glycogen synthase and the control of glycogen synthesis. *Proc. Natl. Acad. Sci. U.S.A.* **92**, 8535–8542 (1995).

45. H. Kacser, J. W. Porteous, Control of metabolism: What do we have to measure? *Trends Biochem. Sci.* **12**, 5–14 (1987).

46. D. A. Fell, H. M. Sauro, Metabolic control and its analysis: Additional relationships between elasticities and control coefficients. *Eur. J. Bioche.* **148**, 555–561 (1985).

47. N. Kumashiro et al., Targeting pyruvate carboxylase reduces gluconeogenesis and adiposity and improves insulin resistance. *Diabetes* **62**, 2183–2194 (2013).

48. S. C. Hung, R. R. Pochampally, S. C. Chen, S. C. Hsu, D. J. Prockop, Angiogenic effects of human multipotent stromal cell conditioned medium activate the PI3K-Akt pathway in hypoxic endothelial cells to inhibit apoptosis, increase survival, and stimulate angiogenesis. *Stem Cells* **25**, 2363–2370 (2007).

49. J. H. Zar, *Biostatistical Analysis* (Prentice-Hall, ed. 2, 1984), chap. 18.

www.manaraa.com